Absorbed doses to water for x-ray dosimetry on a PXI X-RAD 225
Part I – Measurements

A technical document series for CERAD partners in support of

x-ray irradiation of cell cultures and mice.

Statens strålevern
Norwegian Radiation Protection Authority

Absorbed doses to water for x-ray dosimetry on a

PXI X-RAD 225

Part I – Measurements

A technical document series for CERAD partners in support of x-ray irradiation of cell cultures and mice.

Report and analysis: Elisabeth Lindbo Hansen (elisabeth.hansen@nrpa.no)

Measurements: Ingrid Helen Ryste Hauge, Per Otto Hetland, Hans Bjerke

Reference:

Lindbo Hansen E. Absorbed doses to water for x-ray dosimetry on a PXI X-RAD 225.
Teknisk dokument nr. 7. Østerås: Norwegian Radiation Protection Authority, 2015.
Language: English.
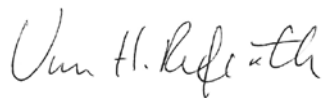
Key words:

Dosimetry. X-ray. Depth dose distribution. Ionization chamber. Water phantom. Film.
Uncertainty.

Abstract:

For a tube potential of 225 kV, current of 10 mA and source-to-surface distance (SSD) of 50 cm,
the absorbed dose rate to water on the central field axis at a depth of 2 g/cm^2 of water in the
21.0 cm×21.0 cm×11.5 cm water phantom was (1.16±0.02) Gy/min. The field diameter at this
SSD was 23 cm and the absorbed dose rate to water near the surface of the phantom was
calculated to (1.18±0.03) Gy/min.

Resymé:

For et rørpotensial på 225 kV, strøm på 10 mA og avstand fra kilde til overflate (SSD) på 50 cm
var den absorberte doseraten til vann i strålefeltets sentralakse i en dybde på 2 g/cm^2 vann i et
21.0 cm×21.0 cm×11.5 cm vannfantom (1.16±0.02) Gy/min. Feltdiameteren ved denne SSD'en
var 23 cm og den absorberte doseraten til vann nær overflaten til fantomet ble beregnet til
(1.18±0.03) Gy/min.

Prosjektleder: Åste Søvik.
Godkjent:

Refseth Unn Hilde, avdelingsdirektør, avdeling overvåkning og forskning

---

Contents

1 Introduction

This report concerns measurements on a PXI X-RAD 225 (Precision X-ray Inc., North Branford, CT) [1] of the absorbed dose to water at a depth of 2 g/cm^2 of water in a 21.0 cm × 21.0 cm × 11.5 cm large water phantom with poly(methyl methacrylate) (PMMA) walls. The measurements were performed with a NE2571 Farmer-type ionization chamber traceable via a transfer ionization chamber to a calorimetric primary standard for absorbed dose at the Physikalisch-Technische Bundesanstalt (PTB) [2]. The X-RAD 225 is a self-contained, single-focus x-ray irradiation system with available tube voltages from 5 to 225 kV located at the Norwegian Institute of Public Health (NIPH). The measurements were performed by the Secondary Standard Dosimetry Laboratory (SSDL) at the Norwegian Radiation Protection Authority (NRPA) and the CERAD Center of Excellence in Environmental Radioactivity in May and September of 2014. The purpose was to characterize the X-RAD 225 in terms of absorbed dose to water to support dose-effect studies performed by CERAD partners from NRPA on cell cultures in Petri dishes. The measurements largely follow the code of practice for medium-energy kilovoltage x-ray beams as defined by the International Atomic Energy Agency (IAEA) in TRS-398 [3]. The lateral dimensions of the water phantom (21.0 cm × 21.0 cm × 11.5 cm) relative to the extent of the field (23 cm at a set source-to-surface distance of 50 cm) are however smaller than those recommended in TRS-398 [3] and the half-value layer (HVL) was determined from measurements in a water phantom for a broad field rather than free-in-air for a collimated beam. The error introduced by this is assessed in the appendix and accounted for in the reported results.

2 Summary of results

For a set potential of 225 kV, a set current of 10 mA and a set source-to-surface distance (SSD) of 50 cm, the absorbed dose rate to water on the central field axis at a depth of 2 g/cm^2 of water in the 21.0 cm × 21.0 cm × 11.5 cm water phantom was found to be (1.16 ± 0.02) Gy/min. Here the uncertainty is the combined standard uncertainty. The beam was filtered through 0.80 mm Be (default) and 0.50 mm Cu (optional). The field diameter at a set source-to-surface distance of 50 cm was found to be 23 cm. For this field size, the absorbed dose rate to water near the surface of the phantom with a set source-to-surface distance of 50 cm, is calculated via percentage depth dose distributions (PDDs) and tissue-air ratios (TARs) in the literature [4, 5] to (1.18 ± 0.03) Gy/min.

3 Theory and background

The current report concerns x-ray beams from a generating potential of 225 kV between a hot cathode and a W anode. The maximal photon energy theoretically expected from such a setup is 225 keV. The potential provides electrons with kinetic energies that are sufficient for ejection of electrons from inner shell orbitals

in W. Characteristic W x-ray lines, including the W K-lines at 58, 59, 67 and 69 keV [6], are therefore present in the x-ray spectrum in addition to the continuous spectrum from bremsstrahlung events.

In the current setup, the beam undergoes filtering through 0.80 mm Be (default) and 0.50 mm Cu (optional), corresponding to mass thicknesses of respectively $x_{Be} = 0.15$ g/cm^2 Be and $x_{Cu} = 0.45$ g/cm^2 Cu [7]. The mass thickness is the product of the thickness with the density of a material. The attenuation of a narrow, collimated beam passing through a material is described by the equation

$$I = I_0 \exp(-(\mu/\rho)x), \tag{1}$$

where I is the attenuated intensity, I_0 the incident intensity and μ/ρ the mass attenuation coefficient [7]. When $(\mu/\rho)x > 3.0$, $I/I_0 < 5.0\%$. For Cu, $(\mu/\rho)_{Cu}x_{Cu} > 3.0$ at photon energies below roughly 30 to 40 keV [7]. About 95% or more of photons with energies below 30 to 40 keV are therefore removed from a hypothetical narrow collimated beam by a 0.50 mm Cu filter. For a set potential of 225 kV and a filtering of 0.50 mm Cu, the fluence weighted mean photon energy is expected to fall roughly in the range from 60 to 100 keV [8].

4 Materials and methods

4.1 The irradiation cabinet

The X-RAD 225 is a self-contained, single-focus x-ray irradiation system designed for use in research laboratories [1]. The irradiation system uses a GE ISOVOLT TITAN 225 generator featuring a W anode. With a focus spot size on the anode of 7.5 mm, the generator has available tube voltages from 5 to 225 kV, tube currents from 0.1 to 45 mA, and exposure set times from 1 to 999 s or from 0.1 to 99.9 min. The maximum tube current at maximum voltage is 13 mA, giving a tube power of $225 \, \text{kV} \cdot 13 \, \text{mA} = 2.9 \, \text{kW}$. Higher powers can result in the anode overheating. The safety interlock cabinet has a stainless steel interior, lead shielding and a laminated steel exterior. A ceramic internal height shelf is used to adjust the source-to-surface distance and features measurement notches with a 1 mm resolution. At a set source-to-surface distance of 30.4 cm the field diameter is specified on the cabinet to be 15.7 cm, at 40.0 cm to be 20.7 cm and at 50.0 cm to be 25.9 cm. These values are checked against Gafchromic EBT film measurements in a later section, where it is found that the actual field diameter at a set source-to-surface distance of 50 cm is 23 cm. A filter holder is provided for optional beam hardening in addition to the inherent default filtration, which is through 0.80 mm Be. In the current report, all measurements were made with a 0.50 mm Cu filter in the filter holder.

4.2 The ionization chamber and the water phantom

A NE2571 Farmer-type ionization chamber in conjunction with a PMMA-enclosed water phantom was used for measuring the absorbed dose to water at a reference depth of $z_{ref} = 2$ g/cm^2 of water. The ionization

chamber has a cavity volume of 0.6 cm^3, a cavity length of 24.0 mm and a cavity radius of 3.2 mm [3]. The chamber wall is 0.065 g/cm^2 of graphite and the central electrode 1.0 mm of Al [3].

The ionization chamber was coupled to a measuring assembly featuring an electrometer with a four-digit or better resolution. The ionization chamber was inserted into a cylindrical cavity in the water phantom whose wall thickness was 2 mm of PMMA. The outer dimensions of the water phantom were 21.0 cm × 21.0 cm × 11.5 cm and the PMMA walls were 0.75 cm thick. The phantom was placed so that the estimated center of the x-ray field was on the ionization chamber axis at the center of the cavity volume, with this point being located at $z_{ref} = 2$ g/cm^2 of water. In order to estimate the half-value layer, plates of respectively 1.0, 1.5 and 2.0 mm Cu were placed on top of the water phantom. The half-value layer was thus determined to be between 1.0 and 1.5 mm Cu, with roughly 1.3 mm Cu being the best estimate obtained by interpolation. The error associated with this non-standard half-value layer determination is assessed in the appendix, where it is found that the true half value layer lies closer to 1.0 than 1.5 mm Cu.

From the measured charge M accumulated over time t, the absorbed dose rate to water is calculated as

$$\dot{D}_w = \left(N_{D,w} \cdot M \cdot k_Q \cdot k_\rho\right)/t. \tag{2}$$

For the NE2571 chamber (serial number 3016), $N_{D,w} = 4.519 \cdot 10^7$ Gy/C at the reference conditions of $T_0 = 20.0$ ^{o}C (293.2 K) and $P_0 = 101.325$ kPa [2]. The factors k_Q and k_ρ provide corrections for deviations in beam quality and air density from the reference conditions. Calculations of absorbed doses and dose rates were performed with the aid of a TRS-398 associated spreadsheet for medium-energy kilovoltage x-ray beams [3, 9]. Here k_Q is estimated from tabulated calibration data, interpolating between values of $k_Q = 0.986$ at a HVL of 0.82 mm Cu and $k_Q = 1.000$ at a HVL of 2.55 mm Cu for the specific chamber utilized [2]. The correction factor for the air density is calculated as

$$k_\rho = (T \cdot P_0)/(T_0 \cdot P), \tag{3}$$

where (T_0, P_0) is the temperature (in K) and pressure at the reference conditions and (T, P) the temperature and pressure at the measurement conditions. In the measurements the ambient air pressure was 102.25 kPa, the temperature 23.3 ^{o}C (296.5 K) and the relative humidity about 50%.

4.3 Gafchromic EBT films

Gafchromic EBT films from Ashland/International Specialty Products (lot #37122-041) [10] were used to estimate the extent of the field in the lateral directions perpendicular to the central beam axis. The films were older than the expiration date recommended by the manufacturer (May, 2009) and were therefore only used for relative assessments of the extent of the field. The exposed films were scanned in transmission mode on an Epson V750 Pro. The net optical density for a pixel in the red channel was obtained as

$$OD_{r,net} = \log_{10}(I/I_0), \tag{4}$$

where I is the transmitted intensity for a pixel in the red channel and I_0 the transmitted intensity for this pixel in the red channel of an unexposed film [11, 12].

4.4   The central axis depth dose distribution

All measurements performed with an ionization chamber in the current report provide the absorbed dose to water at a depth of $z_{ref} = 2$ g/cm^2 of water. Extrapolation to absorbed doses at other depths and for other geometries can be performed either experimentally, or via Monte Carlo radiation transport simulations for example with Geant4 [13-15], which is a toolkit that is expected to perform well in the current exposure scenario [16]. Preliminary estimates based on percentage depth dose distributions (PDDs) and tissue-air ratios (TARs) in the literature [4, 5] are presented in the following chapters. It is assumed that the only factors affecting the ratio of the absorbed dose to water near the surface to the absorbed dose to water at the reference depth are the distance from the source (inverse square law), the attenuation of the primary beam by the phantom, and the scatter from the phantom.

For the purpose of these calculations, field diameters are converted to equivalent square areas [5]. The measured diameter of 23 cm at a set source-to-surface distance of 50 cm is thus converted to an equivalent square area of between 20 cm $\times$ 20 cm and 22 cm $\times$ 22 cm [5]. The latter field dimensions coincide with the borders of the water phantom. For a half-value layer of 1.0 mm Cu and a source-to-surface distance of 50 cm, the backscatter factor (BSF) for a 20 cm $\times$ 20 cm field, also known as the tissue-air ratio (TAR) at zero depth, is 1.487 and the peak scatter factor (PSF), also known as the tissue-air ratio at the depth of dose maximum, 1.589 [5]. The percentage depth dose at a depth of $z_{ref} = 2$ g/cm^2 of water is 98.4% when the source-to-surface distance is 50 cm and the dose profile is normalized to 100.0% near the surface where $z = z_0 = 0$ [5]. The depth of dose maximum at the same conditions is estimated to occur at $z = z_m = 1$ g/cm^2 of water with the absorbed dose to water at z_m being 103.0% of the surface absorbed dose [5].

Formulae exist for conversion of percentage depth doses between different source-to-surface distances [5]. In particular, given a known percentage depth dose $PDD(z, SSD_1, S/F)$ at the depth z for a given source-to-surface distance SSD_1, the percentage depth dose at the same depth but another source-to-surface distance SSD_2 and surface field size S can be calculated as [5]

$$PDD(z, SSD_2, S) = PDD(z, SSD_1, S/F) \cdot (PSF(S/F)/PSF(S)) \cdot F_S^2, \tag{5}$$

where

$$F = ((SSD_1 + z)/SSD_1) \cdot (SSD_2/(SSD_2 + z)) \tag{6}$$

and

$$F_S = ((SSD_1 + z)/(SSD_1 + z_0)) \cdot ((SSD_2 + z_0)/(SSD_2 + z)). \tag{7}$$

4.5 Uncertainty

Uncertainty involves both sample statistics and the estimation of population parameters. In the following, the sample mean $\bar{X}$ of N measures X_i is calculated as [17]

$$\bar{X} = (1/N) \sum_1^N X_i, \tag{8}$$

and the sample standard deviation s_N as [17]

$$s_N = \sqrt{(1/N) \sum_1^N (X_i - \bar{X})^2}. \tag{9}$$

If the sample was drawn from a population then the sample estimate for the population mean μ is obtained as [17, 18]

$$\hat{\mu} = \bar{X}, \tag{10}$$

and the sample estimate for the population standard deviation σ as [17, 18]

$$\hat{\sigma} = \sqrt{(N/(N-1))} \cdot s_N. \tag{11}$$

According to the central limit theorem, the sample estimate for the population mean is itself a normally distributed random variable with mean $\hat{\mu}$ and standard deviation $\hat{\sigma}/\sqrt{N}$ [18]. The result of N measures X_i may therefore be reported as [18, 19]

$$\hat{\mu} \pm \hat{\sigma}/\sqrt{N}, \tag{12}$$

where $\hat{\sigma}/\sqrt{N}$ is the standard uncertainty of the sample estimate of the population mean.

Uncertainty budgets for the calculation of the absorbed dose at the reference depth of $z_{ref} = 2$ g/cm^2 of water and near the surface of the phantom are presented in the appendix.

5 Results and discussion

5.1 The mean measured accumulated charge at the reference depth on the beam axis

The results of measurements with the ionization chamber at the reference depth of $z_{ref} = 2$ g/cm^2 of water in the phantom are presented in Table 1. The set voltage, current and exposure time are user inputs to the irradiation system. The set distance was the distance to the phantom surface as measured on the ruler in the x-ray cabinet. The mean measured accumulated charge was calculated from minimally three repeated measurements at each set point.

Table 1: Mean measured accumulated charge at different set exposure conditions at the reference depth of $z_{ref} = 2$ g/cm^2 of water. The ambient air pressure was 102.25 kPa, the temperature 23.3 °C and the

relative humidity about 50%. *The set distance was the distance to the phantom surface as measured on the ruler in the x-ray cabinet. The uncertainty is the standard uncertainty (equation (12)).*

Set voltage	Set current	Set exposure time	Set distance	Mean measured accumulated charge
[kV]	[mA]	[s]	[cm]	[nC]
225	13	60	30	84.51 ± 0.01
225	13	30	30	41.96 ± 0.02
225	13	30	35	32.03 ± 0.01
225	13	30	40	25.12 ± 0.01
225	13	30	45	20.31 ± 0.01
225	13	30	50	16.646 ± 0.005
225	10	30	50	12.790 ± 0.009
225	7	30	50	8.924 ± 0.008
225	4	30	50	5.085 ± 0.011
225	1	30	50	1.2512 ± 0.0002
225	0.1	30	50	0.2232 ± 0.0002

The measurements for fixed conditions but varying exposure times (see Table 1) indicate a timer offset of 0.4 s, so that a set exposure time of e.g. 30 s corresponds to an actual beam-on exposure estimated to 29.6 s. The timer offset is consistent with the 1 s timer resolution of the X-RAD 225 system, although the uncertainty on the mean measured accumulated charge indicates that the precision on the exposure time is higher but featuring the determined offset. The offset on the set source-to-surface distance relative to the effective distance from the surface to the source focus was found to be -2 cm (see Figure 1), so that a set distance of e.g. 50 cm corresponds to an effective source-to-surface distance of 52 cm.
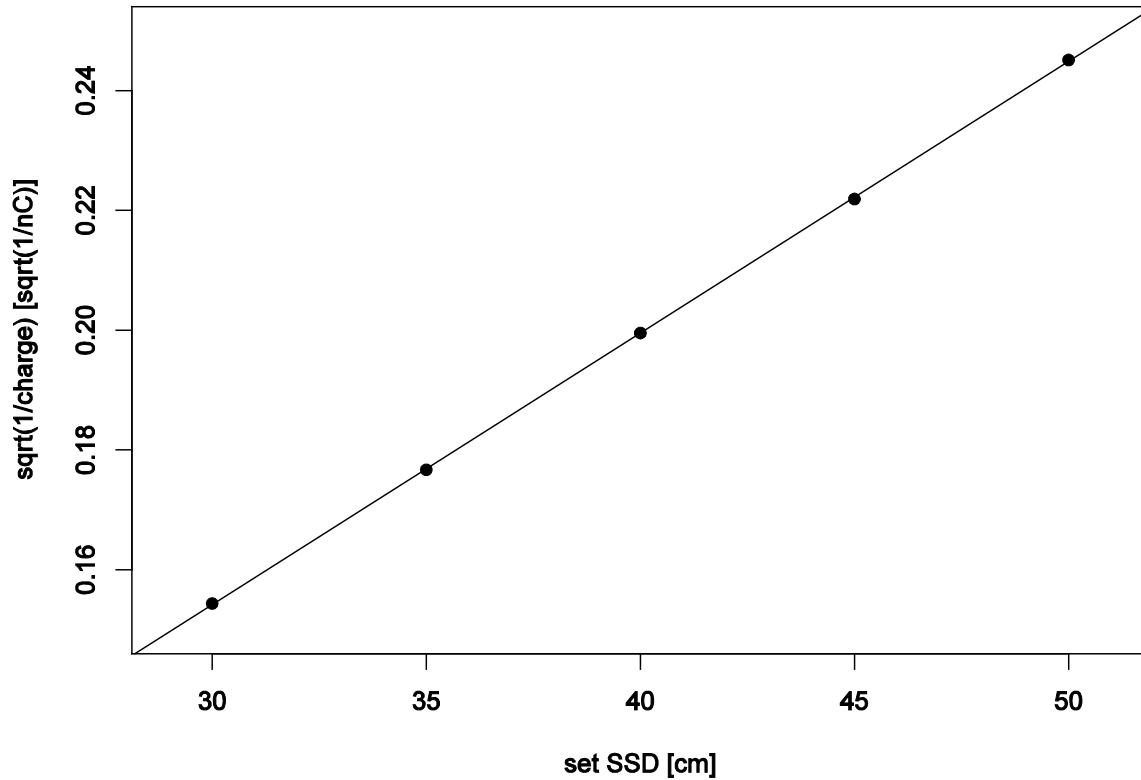
Figure 1: The square root of the inverse of the mean measured accumulated charge plotted versus the set source-to-surface distance (SSD) for a set current of 13 mA *and a set exposure time of* 30 s*. The set distance was the distance to the phantom surface as measured on the ruler in the x-ray cabinet. The effective distance to the source focus is estimated from a linear fit in R [20] of* $\sqrt{1/charge} = a \cdot set\ SSD + b$ *based on the inverse square law which predicts that* $charge = c/(set\ SSD - offset)^2$*. The best estimates for the coefficients were* $a = 1/\sqrt{c} = 4.53 \cdot 10^{-3} \sqrt{(1/nC)}/$cm *and* $b = 1.82 \cdot 10^{-2} \sqrt{(1/nC)}$ *so that the* $offset = -b/a = -4.02$ cm*. Because* 2 cm *of the offset are attributable to the distance from the phantom surface to the depth of measurement, the effective source-to-surface distance is found to be* 2 cm *longer than the set source-to-surface distance.*

5.2 Calculated absorbed dose rates at the reference depth on the beam axis

Calculated absorbed dose rates to water at the reference depth of $z_{ref} = 2$ g/cm^2 of water are presented in Table 2. The details of the calculations are explained in TRS-398 [3] and in an associated spreadsheet for absorbed dose to water calculations for medium-energy kilovoltage x-ray beams [9]. The uncertainties on the absorbed dose rates are calculated from a combined relative standard uncertainty on the absorbed dose of 2% (see appendix), assuming an insignificant uncertainty on both the set and actual exposure times.

11

Table 2: Calculated apparent and actual absorbed dose rates to water at different set exposure conditions at the reference depth of $z_{ref} = 2$ g/cm^2 of water. The apparent dose rate is obtained from the mean measured accumulated charge and the set exposure time. In the actual dose rate the timer offset has been accounted for. The set distance was the distance to the phantom surface as measured on the ruler in the x-ray cabinet. The uncertainty is the combined standard uncertainty (see appendix).

| Set voltage	Set current	Exposure time		Set distance	Calculated absorbed dose rate to water	
		Set	Actual		Apparent	Actual
[kV]	[mA]	[s]		[cm]	[Gy/min]	
225	13	60	59.6	30	3.78 ± 0.08	3.81 ± 0.08
225	13	30	29.6	30	3.75 ± 0.08	3.81 ± 0.08
225	13	30	29.6	35	2.87 ± 0.06	2.91 ± 0.06
225	13	30	29.6	40	2.25 ± 0.04	2.28 ± 0.05
225	13	30	29.6	45	1.82 ± 0.04	1.84 ± 0.04
225	13	30	29.6	50	1.49 ± 0.03	1.51 ± 0.03
225	10	30	29.6	50	1.14 ± 0.02	1.16 ± 0.02
225	7	30	29.6	50	0.799 ± 0.016	0.810 ± 0.016
225	4	30	29.6	50	0.455 ± 0.009	0.462 ± 0.009
225	1	30	29.6	50	0.112 ± 0.002	0.114 ± 0.002
225	0.1	30	29.6	50	0.0200 ± 0.0004	0.0203 ± 0.0004
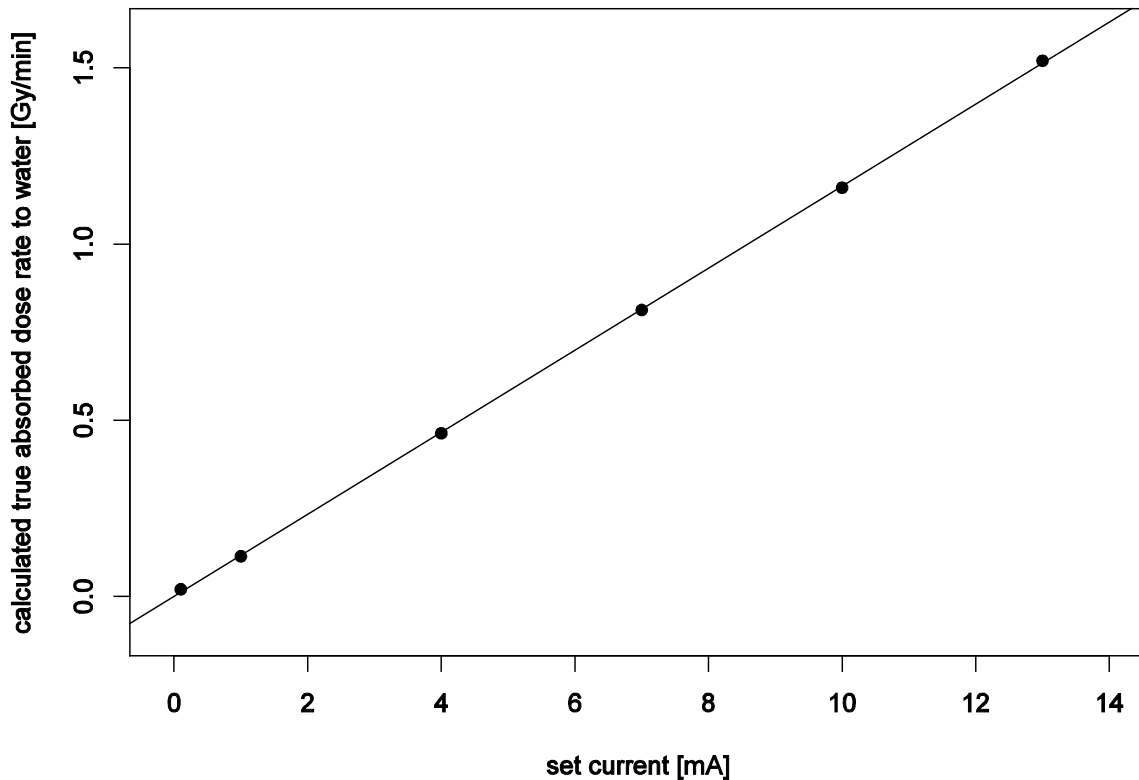
Figure 2: Calculated actual absorbed dose rate to water at a depth of $z_{ref} = 2$ g/cm^2 of water versus the set current for a set source-to-surface distance (SSD) of 50 cm and a set exposure time of 30 s. A linear fit in R [20] of absorbed dose rate $= a \cdot current + b$ gives best estimates for the coefficients of $a = 1.16 \cdot 10^{-1}$ (Gy/min)/mA and $b = 1.47 \cdot 10^{-3}$ Gy/min.

5.3 Field size estimations with Gafchromic EBT film

Gafchromic EBT films from Ashland/International Specialty Products (lot #37122-041) [10] were used to estimate the extent of the field in the lateral directions perpendicular to the central beam axis at a set source-to-surface distance of 50 cm. The field diameter at this source-to-surface distance was found to be 23 cm, with the net optical density across the field being within 90% of the maximum optical density around the central field. The field was found to be well approximated as flat in a 7 cm diameter circular area around the central field axis. A scan of one of the films is shown in the appendix.

5.4 Estimated absorbed dose rates near the surface of the water phantom on the beam axis

Absorbed dose rates to water near the surface of the water phantom can be estimated from percentage depth dose distributions (PDDs) and tissue-air ratios (TARs) in the literature [4, 5]. The first step is to convert

tabulated percentage depth dose distributions for a source-to-surface distance of 50 cm [5] with the help of equations (5-7) to depth dose distributions for a source-to-surface distance of 52 cm. The percentage depth dose at a depth of $z_{ref} = 2$ g/cm^2 of water for a source-to-surface distance of 50 cm of 98.4% for a half-value layer of 1.0 mm Cu, is thus converted to a percentage depth dose for a source-to-surface distance of 52 cm of 98.7%. The dose profile is still normalized to 100.0% at the surface where $z = z_0 = 0$ [5]. The resulting absorbed dose rates to water near the surface of the water phantom for a set source-to-surface distance of 50 cm are reported in Table 3 for set tube currents of 13, 10, 7 and 4 mA.

Table 3: Estimated actual absorbed dose rates to water at the reference depth in the phantom and near the surface of the phantom. The total absorbed dose can be calculated as the actual exposure time multiplied with the actual dose rate. The uncertainty is the combined standard uncertainty (see appendix).

Set voltage	Set current	Exposure time		Set distance	Calculated actual dose rate	
		Set	Actual		At the reference depth	Near the phantom surface
[kV]	[mA]	[s]		[cm]	[Gy/min]	
225	13	30	29.6	50	1.51 ± 0.03	1.53 ± 0.04
225	10	30	29.6	50	1.16 ± 0.02	1.18 ± 0.03
225	7	30	29.6	50	0.810 ± 0.016	0.82 ± 0.02
225	4	30	29.6	50	0.462 ± 0.009	0.468 ± 0.013

6 Recommendations and outlook

6.1 Quality control

Quality control is necessary for all scientific equipment. For the PXI X-RAD 225, a quality control system should be established for periodic measurements of a dose or radiometric quantity in a well-defined reference setup. The measurements should involve a standards-traceable protocol.

6.2 Spectral measurements

The error associated with a non-standard half-value layer determination has been assessed in the appendix and accounted for in the reported results. For a more detailed characterization of the system and to support radiation transport simulations it is recommended that equipment for spectral characterization could be invested in. Some possible options are differently shielded passive integrating dosimeters [21] or sufficiently small double pinhole collimated semiconductor detectors, such as CdTe detectors [22].

6.3 Dosimetry for cell cultures and mice

The purpose of the current work has been to characterize the X-RAD 225 in terms of absorbed dose to water to support dose-effect studies performed by CERAD partners from NRPA on cell cultures in Petri dishes. Special considerations necessary for the exposure of cell cultures will be discussed in a separate report. A third report will deal with exposures of mice.

7 Appendix

7.1 Evaluation of the error introduced by a non-standard HVL determination

A simplified Geant4 [13-15] model of the irradiation cabinet was built to investigate the error introduced by a non-standard determination of the half-value layer (HVL). The model was used to simulate the specific energy imparted to water at 1 versus 2 g/cm^2 of water, and to simulate the actual measurements of the half-value layer (in poor geometry) and ideal measurements of the half-value layer (in good geometry). For the poor geometry simulations, Cu sheets of varying thickness were placed on top of a 21.0 cm $\times$ 21.0 cm $\times$ 11.5 cm large water phantom and the specific energy tallied to water at 2 g/cm^2 of water. In the good geometry simulations, two lead collimators narrowed the beam and the specific energy was tallied to a block of lead placed free in air. All simulations were performed with the G4EmStandardPhysics_option4 physics list, with a geometrically realistic but monoenergetic beam diverging from the source focus. The simulated water had a density of 1.00 g/cm^3 and a mean excitation energy of 78 eV.

Validation runs at a monoenergetic exposure of 80 keV reproduced the measured data at 2 g/cm^2 of water with good accuracy across the relevant range of effective distances to the source focus. Data from Tables 4 and 5 demonstrate that the ratio of the mean simulated specific energy imparted to water at 1 relative to 2 g/cm^2 of water for photons of energy 80 keV corresponds well with tabulated data for x-rays beams with a half-value layer of 1.0 mm of Cu [5]. The variability of this ratio across the range from 40 to 200 keV, which covers the expected spectrum of the x-rays in the actual exposures after the beam-hardening Cu filter, is relatively small.

In Tables 4 and 5, it is found that the non-standard determination of the half-value layer in poor geometry overestimates this quantity. This tendency is least pronounced at the lowest simulated beam energy of 40 keV where photoelectric absorption constitutes 93% of the total attenuation cross section in Cu [23], and most pronounced at 200 keV where photoelectric absorption makes up 22% of the total attenuation cross section and incoherent (Compton) scattering dominates [23]. In an actual broad beam exposure, this means that a Cu filter hardens a soft beam by selectively absorbing at the lower energies but can soften a hard beam by contributing a dose from lower energy photons scattered into the detecting volume. The ratio of the half-value layer simulated for a broad beam and poor geometry exposure to that calculated for an ideal exposure ranges from 1.1 at 40 keV to 1.2 at 80 keV and 1.7 at 200 keV. The simulations therefore

indicate that the half-value layer of 1.3 mm Cu estimated from the poor geometry measurements corresponds to a half-value layer which for a good geometry setup would be closer to 1.0 than to 1.5 mm Cu.

Table 4: Data for $1 \cdot 10^9$ simulated photons at the specified energies for sensitive detectors of dimensions 10.0 mm $\times 10.0$ mm $\times 4.00$ mm, having volumes of 0.400 cm^3 of water at a density of 1.00 g/cm^3. The volumes were located on the central axis of a 21.0 cm $\times 21.0$ cm $\times 11.5$ cm large water phantom placed at an effective distance from the surface to the source focus of 50.00 cm. The uncertainty on the simulated ratio of dose quantities is the standard uncertainty (equation (12)) obtained from a Type A statistical evaluation.

Energy	Ratio of dose quantities at 1 cm versus 2 cm depth		HVL		
	Simulated	Tabulated, for a HVL of 1.0 mm Cu (from [5])	Simulated, poor geometry	Simulated, good geometry	Theoretically, good geometry (from [23])
[keV]	[1]	[1]	[mm Cu]		
80	1.046 ± 0.002	1.05	1.2	1.1	1.0

Table 5: Data for $1 \cdot 10^9$ simulated photons at the specified energies for sensitive detectors of dimensions 10.0 mm $\times 10.0$ mm $\times 4.00$ mm, having volumes of 0.400 cm^3 of water at a density of 1.00 g/cm^3. The volumes were located on the central axis of a 21.0 cm $\times 21.0$ cm $\times 11.5$ cm large water phantom placed at an effective distance from the surface to the source focus of 52.02 cm. The uncertainty on the simulated ratio of dose quantities is the standard uncertainty (equation (12)) obtained from a Type A statistical evaluation.

Energy	Ratio of dose quantities at 1 cm versus 2 cm depth		HVL		
	Simulated		Simulated, poor geometry		Theoretically, good geometry (from [23])
[keV]	[1]		[mm Cu]		
40	1.123 ± 0.006		0.17		0.16
80	1.036 ± 0.004		1.2		1.0
200	1.058 ± 0.005		8.7		5.0

7.2 Uncertainty budgets

Tables 6 and 7 present uncertainty budgets for the determination of absorbed dose to water at the reference depth in water and near the surface of the water phantom.

Table 6: Uncertainty budget for the absorbed dose to water at $2\,\mathrm{g/cm^2}$ of water.

Quantity or procedure	Relative standard uncertainty
	[%]
$N_{D,w} \cdot k_{Q0}$ calibration of NE2571 Farmer chamber at PSDL [2]	1.1
Long term stability of NE2571 Farmer chamber	0.2
Establishment of reference conditions during measurement [3]	1.0
Correction for influence quantities k_ρ [3]	0.8
Beam quality correction k_Q [3]	1.0
Combined relative standard uncertainty	2.0

In section 5.4, the percentage depth dose at a depth of $z_{ref} = 2\,\mathrm{g/cm^2}$ of water for a source-to-surface distance of 50 cm of 98.4% for a half-value layer of 1.0 mm Cu, was converted to a percentage depth dose for a source-to-surface distance of 52 cm of 98.7%. For half-value layers of 0.5, 1.5 or 2.0 mm Cu, this value is respectively 93.5%, 99.6% or 99.2% [5]. Taking into account that the non-standard determination of the half-value layer in the measurements introduces an error which was corrected for in the previous section of the appendix, the best estimate for the true half value layer is 1.0 mm Cu. Assuming a rectangular distribution for the probability of the percentage depth dose at $z_{ref} = 2\,\mathrm{g/cm^2}$ of water falling in the interval from 93.5% to 99.6%, the estimated relative standard uncertainty on the absorbed dose near the surface of the phantom from uncertain percentage depth dose distributions becomes 1.9% [25]. This is a conservative estimate.

Table 7: Uncertainty budget for the absorbed dose to water near the surface of the phantom.

Quantity or procedure	Relative standard uncertainty
	[%]
Determination of the absorbed dose to water at $2\,\mathrm{g/cm^2}$ of water	2.0
Percentage depth dose distributions from tabulated rather than actual data	1.9
Combined relative standard uncertainty	2.8

7.3 Raw Gafchromic EBT image

Figure 3: Raw Gafchromic EBT image showing the field relative to the marks present on the irradiation shelf in the cabinet.

8 Acknowledgements

9 References

1.	Precision X-Ray, X-RAD 225 Series. [cited 02/10/2014], http://pxinc.com/products/cabinet-irradiators/x-rad-225-series/

2.	PTB, Calibration Certificate for NE2571 ionization chamber with serial number 3016, Calibration mark PTB 60037-10: Braunschweig (2010).

3.	IAEA, Absorbed Dose Determination in External Beam Radiotherapy: An International Code of Practice for Dosimetry based on Standards of Absorbed Dose to Water. IAEA TRS-398 (2006).

4.	R. Hill, Z. Mo, M. Haque, and C. Baldock, An evaluation of ionization chambers for the relative dosimetry of kilovoltage x-ray beams. Med. Phys. 36 (9), 3971 (2009).

5.	E.G.A. Aird, J.E. Burns, M.J. Day, S. Duane, T.J. Jordan, A. Kacperek, S.C. Klevenhagen, R.M. Harrison, S.C. Lillicrap, A.L. McKenzie, W.G. Pitchford, J.E. Shaw, and C.W. Smith, Central Axis Depth Dose Data for Use in Radiotherapy. British Journal of Radiology Supplement 25 (1996).

6.	R.D. Deslattes, E.G. Kessler Jr., P. Indelicato, L. de Billy, E. Lindroth, J. Anton, J.S. Coursey, D.J. Schwab, C. Chang, R. Sukumar, K. Olsen, and R.A. Dragoset, X-ray Transition Energies (version 1.2), National Institute of Standards and Technology: Gaithersburg, MD (2005).

7.	J.H. Hubbell and S.M. Seltzer, Tables of X-Ray Mass Attenuation Coefficients and Mass Energy-Absorption Coefficients (version 1.4), National Institute of Standards and Technology: Gaithersburg, MD (2004).

8.	F. Verhaegen, A.E. Nahum, S.V.d. Putte, and Y. Namito, Monte Carlo modelling of radiotherapy kV x-ray units. Phys. Med. Biol. 44 (7), 1767 (1999).

9.	IAEA, Dosimetry Codes of Practice and Spreadsheets. [cited 27/05/2014], http://www-naweb.iaea.org/nahu/DMRP/codeofpractice.html

10.	Ashland, Gafchromic radiotherapy films. [cited 02/10/2014], http://www.ashland.com/products/gafchromic-radiotherapy-films

11.	A. Mauring, Radiokromisk film for kontroll av strålefelt: Protokoll for praktisk bruk og behandling av GafChromic EBT til dosimetriformål innen stråleterapi, in Strålevernsrapport, Statens Strålevern: Østerås (2009).

12.   M.J. Butson, P.K.N. Yu, T. Cheung, and P. Metcalfe, Radiochromic film for medical radiation dosimetry. Mat. Sci. Eng. R 41 (3–5), 61 (2003).

13.   S. Agostinelli, et al., Geant4 - a simulation toolkit. Nucl. Instr. Meth. Phys. Res. A 506 (3), 250 (2003).

14.   J. Allison, et al., Geant4 developments and applications. IEEE Trans. Nucl. Sci. 53 (1), 270 (2006).

15.   S. Incerti, et al., Comparison of GEANT4 very low energy cross section models with experimental data in water. Med. Phys. 37 (9), 4692 (2010).

16.   C.C. Guimarães, M. Moralles, and E. Okuno, Performance of GEANT4 in dosimetry applications: Calculation of X-ray spectra and kerma-to-dose equivalent conversion coefficients. Radiat. Meas. 43 (9–10), 1525 (2008).

17.   C. Rose and M.D. Smith, Mathematical Statistics with Mathematica. Springer Texts in Statistics. New York: Springer-Verlag (2002).

18.   J.L. Devore and K.N. Berk, Modern Mathematical Statistics with Applications. 2nd ed. Springer Texts in Statistics, ed. G. Casella, et al., New York: Springer-Verlag (2012).

19.   BIPM, IEC, IFCC, ILAC, ISO, IUPAC, IUPAP, and OIML, Evaluation of measurement data - Guide to the expression of uncertainty in measurement (GUM 1995 with minor corrections), in JCGM 100 (2008).

20.   R.C. Team, R: A language and environment for statistical computing. http://www.R-project.org/

21.   R. Nolte, R. Behrens, M. Schnürer, A. Rousse, and P. Ambrosi, A TLD-Based Few-Channel Spectrometer for X-Ray Fields with High Fluence Rates. Radiat. Prot. Dosim. 84 (1-4), 367 (1999).

22.   AMPTEK, CdTe Application Note: Characterization of X-ray Tubes. [cited 25/03/2015], http://www.amptek.com/cdte-application-note-characterization-of-x-ray-tubes/

23.   M.J. Berger, J.H. Hubbell, S. Seltzer, M., J. Chang, J.S. Coursey, R. Sukumar, D.S. Zucker, and K. Olsen, XCOM: Photon Cross Sections Database (version 1.5), National Institute of Standards and Technology: Gaithersburg, MD (2010).

Statens strålevern
Norwegian Radiation Protection Authority